Electromagnetic Analysis of Forces and Torques on the Baseline and Enhanced ITER Shield Modules due to Plasma Disruption

Joseph D. Kotulski, Rebecca S. Coats, Michael F. Pasik, and Michael Ulrickson

***Abstract*—An electromagnetic analysis is performed on the ITER shield modules under different plasma-disruption scenarios using the OPERA-3d software. The models considered include the baseline design as provided by the International Organization and an enhanced design that includes the more realistic geometrical features of a shield module. The modeling procedure is explained, electromagnetic torques are presented, and results of the modeling are discussed.**

***Index Terms*—Eddy-current analysis, electromagnetic-force computation, ITER.**

I. Introduction

The electromagnetic forces that occur due to plasma disruption are an important consideration in the design of the ITER device. Many different analyses with varying assumptions have been completed by a number of domestic agencies. To help standardize the different analyses, the ITER Organization (IO) has defined geometry, plasma-disruption scenarios, and a protocol for presenting the different results [1].

The purpose of this paper is to present and discuss the results of the electromagnetic benchmarking analysis completed by the U.S. team as prescribed by the IO. This geometry, baseline design, consists of a 40° sector of the device and includes the inner vacuum vessel, divertor assembly, port plugs, and simplified shield modules.

An additional model of shield module 5 was considered with design enhancements including cooling holes and additional eddy-current slits. These results are compared with the baseline design.

A. Geometry

The geometry of the simulated ITER device is shown in Fig. 1. Some key features of this model will now be stated. First, the shield modules are simplified, which implies that they have eddy-current slits but no cooling holes. The placement and depth of the slits have not been optimized. In addition, they are electrically isolated from each other and the vacuum vessel. Finally, symmetry is used so that even though a 40° sector is modeled, it is electromagnetically equivalent to the actual device. From Fig. 1, the single lower port on the vacuum vessel reveals why a 40° sector was modeled—its symmetry is repeated every 40°.

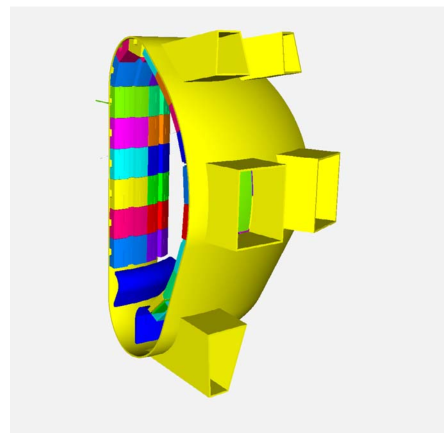

Fig. 1. Forty-degree sector of the ITER device.

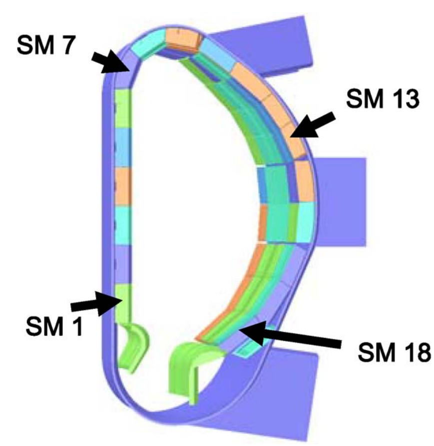

Fig. 2. Shield-module numbering scheme.

Before the results are presented and discussed, some terms need to be defined. The modules are labeled starting from the inboard to the outboard, as shown in Fig. 2.

This numbering is in the poloidal direction of the machine, and additional numbers are added to identify the modules in the toroidal direction. For example, for shield module 1, there would be SM_01_01 and SM_01_02, i.e., shield module 1 in the first and second toroidal positions, respectively. This is shown in Fig. 3 for shield module 18.

Manuscript received July 13, 2009; revised November 18, 2009. First published February 22, 2010; current version published April 9, 2010.

The authors are with the Sandia National Laboratories, Albuquerque, NM 87185 USA (e-mail: jdkotul@sandia.gov).

Color versions of one or more of the figures in this paper are available online at http://ieeexplore.ieee.org.

Digital Object Identifier 10.1109/TPS.2010.2041364

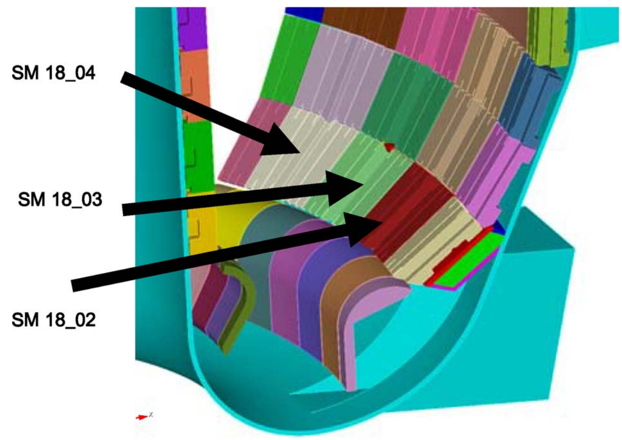

Fig. 3. Numbering scheme for shield module 18.

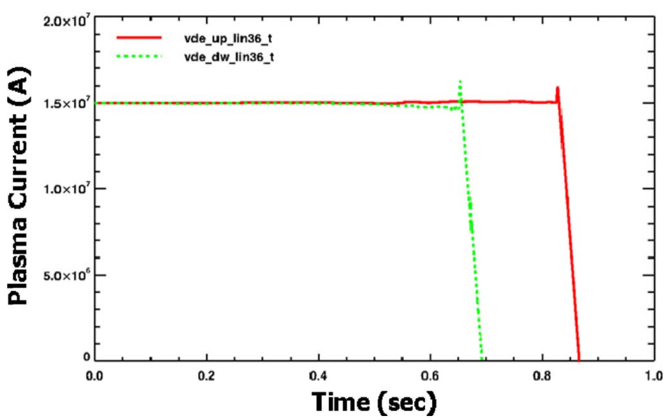

Fig. 4. Total plasma currents for vertical up/down disruption event.

B. Plasma-Disruption Currents

The excitation currents in the device are modeled from the DINA simulations for the particular plasma-disruption event [2]. They include six central solenoid coils, six poloidal field coils, and an axial current (to simulate the toroidal field coil) [3]. The plasma currents are modeled by 100 loops with currents that vary with time but are stationary in space—equivalent to the plasma current in the DINA simulations.

There are three basic disruption scenarios prescribed by the IO, and these include the major disruption (MD UP); vertical displacement event (VDE), upward; and VDE, downward. The variations to these events are due to the manner of decay of the total plasma current after thermal quench. For the analyses presented in this paper, the total plasma current will have a linear current decay. The behavior of the total plasma current for each disruption has the same features—a constant current phase, a thermal quench of the current followed by an increase in current, and then, a linear decay. The total plasma current for two disruption events is shown in Fig. 4. The disruption event not shown in Fig. 4 is the MD UP event which has the same character described except that thermal quench occurs at 8 ms and the plasma current goes to zero at 50 ms.

C. Solution Method

The simulations are performed with the Opera-3d software [4]. This software has a number of features needed for the electromagnetic analysis. First, symmetry can be used, second, the current excitations (from the coils and plasma disruptions) do not depend on the mesh, and finally, the results can be exported for use in software designed for mechanical stress calculations.

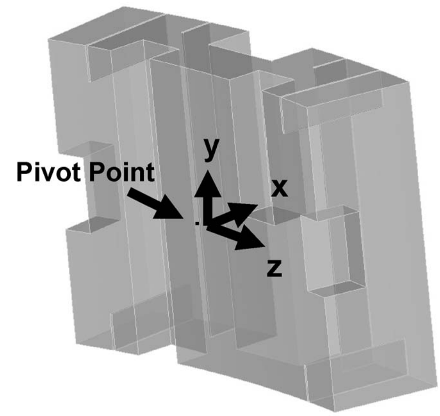

Fig. 5. Pivot location for torque computation (local coordinate axis).

A number of different mesh densities were used for the shield modules to allow the examination of the numerical convergence of the solution for one disruption case. The modules were meshed with tetrahedral elements with average edge lengths of 40, 30, and 20 mm for the coarse to the fine mesh density, respectively. Once the solution for a particular disruption was obtained, the net forces and torques for each module were calculated. The torques were calculated using the pivot points and the coordinate system defined by the IO. Once the torques are calculated, the forces on the shield mounts can be calculated. The results of the force computation are computed at the centroid of the elements that comprise a module and can then be exported to files ready for mechanical analysis. It should be noted that, for the model in Fig. 1, there are 56 separate shield modules.

II. Results

The torque reference points have been prescribed by the IO. These are located between the projections of the four shield-mount points to the vertical midplane of the module. The local coordinate system is defined at this point for each module. The x-axis is the radial direction (toward the center of the machine), the y-axis is in the vertical direction, and the z-axis points in the clockwise direction when viewed from the top of the machine (Fig. 5).

The effect of the lower port of the vacuum vessel on the torque calculations is now considered. This is examined for the module nearest the port (module 18) for the VDE down disruption event. This event is used since the plasma moves toward the lower shield modules on the outboard side of the machine (shield modules 17 and 18) and should accentuate the effect of the lower port on the torque calculations. A comparison of the x-, y-, and z-directed torques for shield modules 18_02, 18_03, and 18_04 is shown in Figs. 6–8, respectively.

Note that the timescale for the figures begins at 0.65 s—the onset of plasma disruption (see Fig. 4).

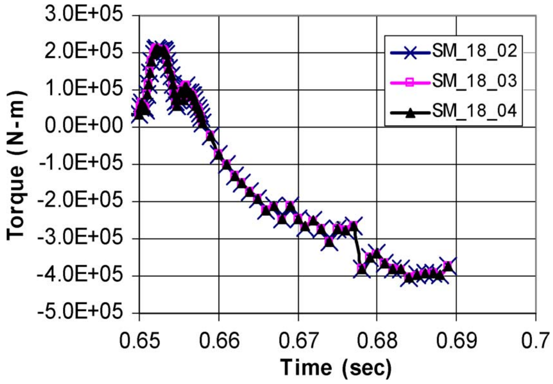

Fig. 6. x-directed torque for shield module 18 for the VDE down disruption case.

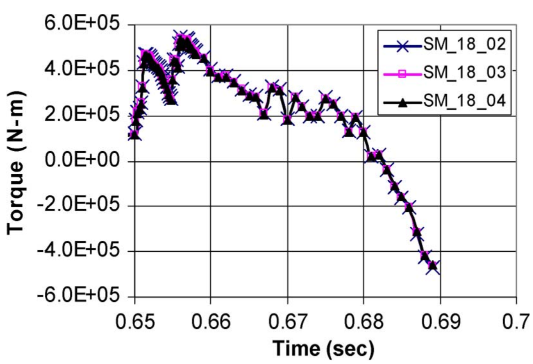

Fig. 7. y-directed torque for shield module 18 for the VDE down disruption case.

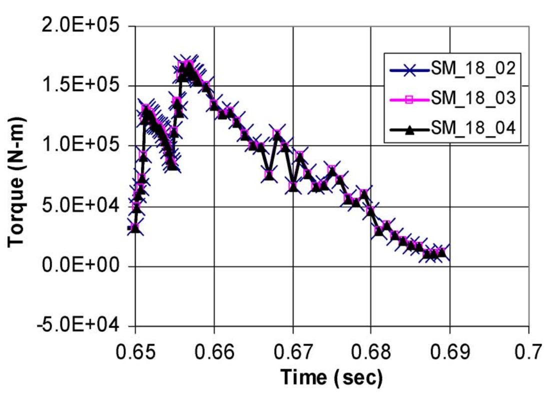

Fig. 8. z-directed torque for shield module 18 for the VDE down disruption case.

As can be seen in the preceding figures, the effect of the asymmetry because of the port has little effect on the torque calculations on the shield module in the proximity of the port. This allows one to reduce the angular sector, simplify the model, reduce the mesh density, and decrease the solution time.

The next step is to investigate the variation in mesh density within the shield modules, which reveals the numerical convergence property of the modeling procedure. Attention is focused on shield module 5 and three different mesh densities. They correspond to 40, 30, and 20 mm, which are the average edge lengths of a tetrahedron. This will be examined for the MD UP case with linear decay. Some of the largest electromagnetic forces are experienced by shield module 5 for this disruption case. The largest torque is in the y-direction, and those results are shown in Fig. 9.

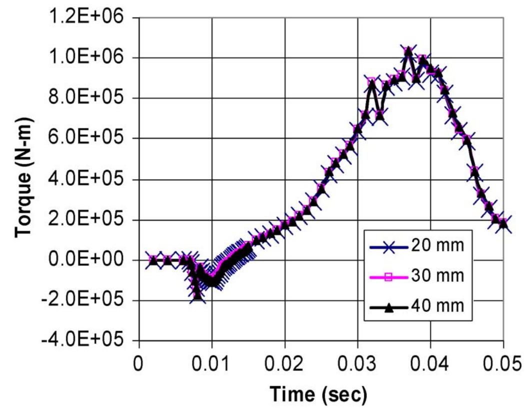

Fig. 9. y-directed torque for shield module 5 for the MD UP case for different module mesh densities.

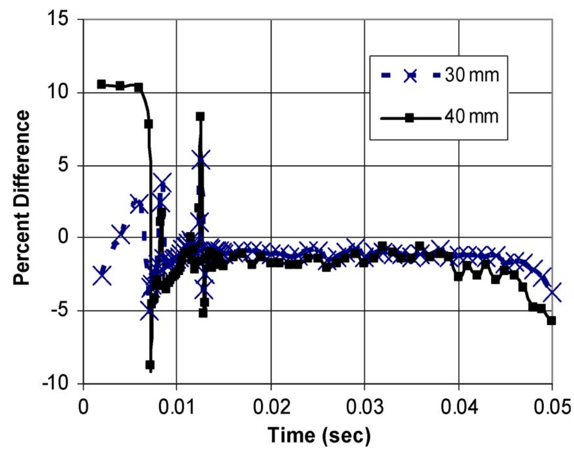

Fig. 10. Percent difference for shield module 5, y-directed torque, for the MD UP case for different module mesh densities.

Again, to the scale of the graph, the results for the three different mesh densities show good agreement. This shows that numerical convergence is acceptable with the coarser mesh density, thus verifying the original assumptions. To be more precise, a percent difference is defined

$$\boldsymbol{PD} = \frac{\boldsymbol{T}_{\boldsymbol{y}}^{r} - \boldsymbol{T}_{\boldsymbol{y}}^{20}}{\boldsymbol{T}_{\boldsymbol{y}}^{20}}. \tag{1}$$

The superscript r refers to the mesh resolution (30 or 40), and $\boldsymbol{T}_{\boldsymbol{y}}^{r}$ is the y-directed torque at the mesh resolution. The results for this error metric are shown in Fig. 10.

Fig. 10 shows that the maximum error is about 11% but occurs before the onset of the plasma disruption. The torque should be zero but some numerical noise is present, giving nonzero but relatively small torque values (about 1900 $\mathrm{N} \cdot \mathrm{m}$).

The final results combine all of the modules and different disruption cases considered in this paper. For each disruption case, the maximum torque at a particular instant of time was identified for each module and then converted to radial (or x-directed) loads. These results, together with the maximum permissible loads, are shown in Fig. 11. These vary with position due to the spatial distribution of the plasma-disruption events.

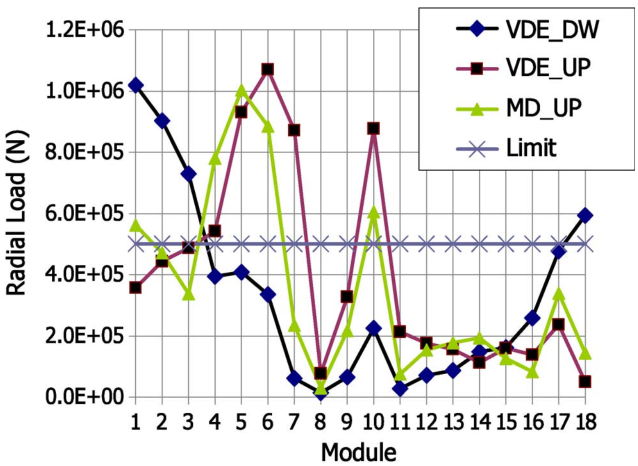

Fig. 11. Maximum radial loads for each shield module for each disruption case.

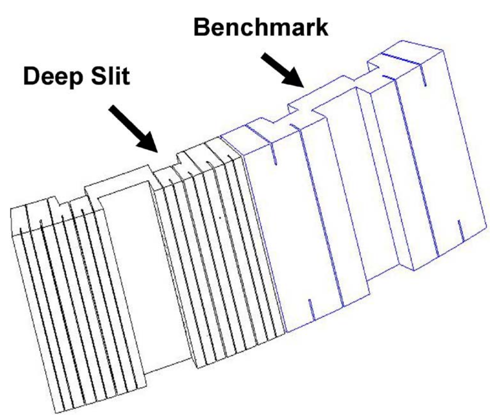

Fig. 12. Improved eddy-current slits for shield module 5.

III. Effect of Design Enhancements

The previous data (shown in Fig. 11) reveal that for a number of shield modules, the radial (x-directed) loads exceed the maximum allowable load. It has to be remembered, however, that the geometry for the baseline shield modules was not optimized for the placement and configuration of the eddy-current slits and did not contain the necessary cooling holes. The purpose of this phase of the analysis is to examine the effect of these two modeling enhancements. The focus of attention will be shield module 5, for disruption case MD UP; for this case, the maximum axial load for the benchmark analysis is above the allowable limit (see Fig. 11). The electromagnetic model for this analysis consisted of a 20° sector and nearby shield modules.

The first enhancement is the inclusion of an improved eddy-current-slit configuration and is shown in Fig. 12.

Fig. 12 shows the improved slit design next to the benchmark which has been rotated for comparison. The slit width for the baseline module was 8 mm, while the enhanced design had slit widths of 5 and 8 mm. The placement and the depth of the slits have also been changed. The second design enhancement is the addition of cooling holes. This addition to the module reduces the volume of steel—the benchmark model was solid. A view of this model that includes cooling holes is shown in Fig. 13.

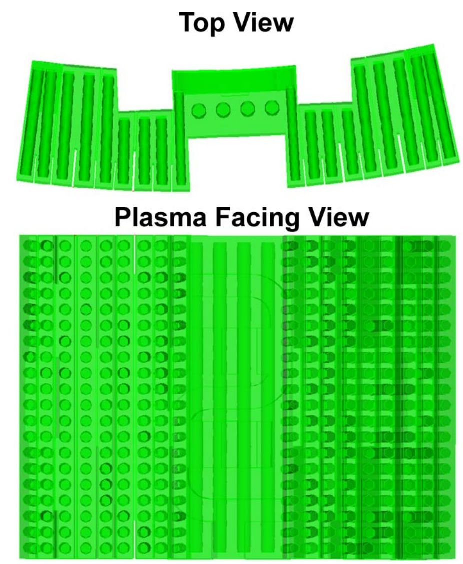

Fig. 13. Cooling-channel locations for shield module 5.

Note that the cooling holes or channels do not form complete circuits, and therefore, the model is an electromagnetic model and is not valid for fluid-flow analysis.

The stainless-steel volumes for the solid and cooling-hole modules are 0.37 and 0.27 m^3, respectively. This is a volume reduction of 27%. The maximum radial (x-directed) load computed for shield module 5 with deep slits and cooling holes was 253 kN. The maximum radial (x-directed) load for the benchmark model can be seen in Fig. 10 to be nearly 1000 kN, and therefore, a reduction of nearly 75% is achieved, which is below the allowable axial load for that module. Clearly, the reduction of the forces depends not only on the reduction in volume but also on the placement of the cooling holes and eddy-current slits.

IV. Conclusion

The electromagnetic forces and torques produced in the ITER shield modules have been considered for three different plasma-disruption scenarios. A number of observations useful in the future modeling of the device have been identified. The first is concerned with the angular sector that was modeled. A 40° sector was chosen due to symmetry considerations with regard to the vacuum vessel. The results presented in this paper clearly show that the additional port in the vacuum vessel does not affect the results for the shield modules near the port. For this reason, a smaller angular model can be used without compromising the accuracy of the simulation as long as the electromagnetic modeling of the shield modules is not changed.

In addition, the numerical convergence of the modeling was also addressed by considering different mesh densities used for the shield modules. Again, very promising results were obtained. The higher density meshed models did not significantly change the calculated results. The lower density meshed model provides not only accurate results but also results that could now be obtained in a more timely fashion due to the reduced model size. The element counts for the 20-, 30-, and 40-mm tetrahedron sizes were 32, 15.5, and 10.8 million elements, respectively. The solution times for the 20-, 30-, and 40-mm tetrahedron sizes were 50, 23, and 13 days, respectively.

The results also reveal that large axial loads are present on a number of shield modules. This has to be taken in the proper context since the EM benchmark geometry was an initial design and not the final design. To help address this issue, a selected shield module was chosen and analyzed. This shield module included a number of design enhancements consisting of additional eddy-current slits and cooling holes. The results show a substantial reduction in the axial load for this module of approximately 75%. This clearly shows the need for the careful modeling of shield modules to more accurately determine the electromagnetic loads due to plasma disruption. Additional analyses have been completed on a select number of modules to identify optimal eddy current reducing slits, the inclusion of cooling holes, and the first wall assembly for a variety of plasma-disruption cases. These have been reported to the IO and will be published at a later time.

Acknowledgment

Sandia National Laboratories is a multiprogram laboratory operated by Sandia Corporation, a Lockheed Martin Company, for the U.S. Department of Energy's National Nuclear Security Administration under Contract DE-AC04-94AL85000.

References

[1] V. Rozov, *Blanket EM Benchmarking Analyses Protocol*, May 2008. ITER_D_2E6P88_v1_0.
[2] H. Fujieda and M. Sugihara, *Initial Equilibrium for Disruption Simulations With the DINA Code*, Feb. 2008. ITER_D_29N7RG_v1_0.
[3] J. D. Kotulski, R. S. Coats, and M. F. Pasik, "Electromagnetic analysis of transient disruption forces on the ITER shield modules," *Fusion Eng. Des.*, vol. 83, no. 7/9, pp. 1068–1071, Dec. 2008.
[4] *OPERA-3d Users Guide*, Cobham Techn. Services, Vector Fields Softw., Aurora, IL, 2008.

Joseph D. Kotulski received the B.S., M.S., and Ph.D. degrees in electrical engineering from the University of Illinois, Chicago, in 1975, 1977, and 1983, respectively.

He is currently with Sandia National Laboratories, Albuquerque, NM, as a Principal Member of the technical staff. His research interests include computational electromagnetics, advanced solver technology applied to numerical techniques in electromagnetics, and high-performance computing.

Rebecca S. Coats received the B.S. degree in mechanical engineering from the University of Arizona, Tucson, in 1981 and the M.S. degree in mechanical engineering from Stanford University, Stanford, CA, in 1982.

Since 1982, she has been with the Pulsed Power Sciences Center, Sandia National Laboratories, Albuquerque, NM, working in the area of computational electromagnetics and plasma physics.

Michael F. Pasik received the B.S.E.E. degree from Purdue University, West Lafayette, IN, in 1988 and the M.S.E.E. and Ph.D. degrees from the University of Arizona, Tucson, in 1991 and 1993, respectively.

Since 1993, he has been with Sandia National Laboratories, Albuquerque, NM, where he is currently a Principal Member of the technical staff. His areas of interest include computational electromagnetics, high-performance computing, and object-oriented software design.

Michael Ulrickson received the B.S. degree in physics from Michigan State University, East Lansing, in 1969 and the Ph.D. degree in nuclear physics from Rutgers University, Piscataway, NJ, in 1975.

His research of carbon-based materials for the plasma facing components for the Tokamak Fusion Test Reactor (TFTR) led to the selection of carbon fiber composite as the preferred plasma facing material. He was a member of the Deuterium-Tritium Materials Physics Group that successfully predicted the tritium retention during DT experiments on TFTR. After 18 years with PPPL, he joined Sandia National Laboratories, Albuquerque, NM, to manage the Fusion Technology Department. From 1993 to 1998, he coordinated the U.S. plasma facing component research supporting the International Thermonuclear Experimental Reactor (ITER) and was the Task Area Coordinator for the international research and development effort on plasma facing components for ITER. He has been Area Coordinator for the U.S. plasma facing component contribution to the ITER project since 2003.

Dr. Ulrickson was the recipient of the Fusion Power Associates Excellence in Fusion Engineering Award in 1988 for his "very important contributions to fusion engineering and in recognition of impressive leadership qualities." In 1995, he was the recipient of a certificate of merit from the Office of Fusion Energy at the Department of Energy and the ITER Home Team for his "outstanding performance on behalf of the U.S. ITER Home Team in the field of divertor development and coordination of the four party R&D effort." He was a member of the Burning Plasma Assessment Panel organized by the National Academy of Sciences to determine the readiness of fusion energy research to undertake a burning plasma experiment during 2003 and 2004.